Mixing in an Arctic Fjord

R. G. PERKIN AND E. L. LEWIS

Frozen Sea Research Group, Institute of Ocean Sciences, Sidney, British Columbia, V8L 3S2 Canada

(Manuscript received 28 December 1977, in final form 5 May 1978)

ABSTRACT

Measurements made in Cambridge Bay, N.W.T., during the winter show that the breaking of internal waves on the shore influences downward salt transport from the homogeneous surface layer produced by saline convection beneath sea ice during growth. Denser water from the shallows, where the depth of this convective layer is limited by the sea bed, flows down the slope to the layer interface contour where the breaking waves introduce turbulence aiding mixing of the convecting water into the lower layer.

Away from the boundaries entrainment of salt from the lower to the upper mixed layer is aided by the internal waves on the interface. These two salt transports, downward at the boundaries upward over the basin, produce horizontal salinity gradients which overall make water in the shallows less saline than the surface layer of the basin. The energies available for these mixing processes are estimated.

1. Introduction

Due to the surface ice cover, mixing in arctic fjords occurs in the absence of wind for the greater part of the year. This, combined with the cessation of estuarine circulation, allows the study of processes which may be masked in fjords at lower latitudes. Major sources of energy for mixing are salt rejection during ice growth, water movements induced by tides or atmospheric pressure changes, and upwelling produced by the melting at depth of icebergs or floating glacial tongues. The last possibility will not be considered further in this paper as the fjord of our study (Cambridge Bay, N.W.T.) does not contain any large ice masses.

Salt rejection by sea ice during growth has been the subject of many studies, one of the most recent being that by Eide and Martin (1975) whose laboratory observations supplemented those made in the field by Lake and Lewis (1970). The vertical circulation associated with this salt flux at the ice/water interface was investigated by Zubov (1943) who assumed that all the potential energy available was dissipated in turbulence during the mixing process. In contrast Kraus and Turner (1967) made calculations based on the premise that the kinetic energy available allowed convecting water to penetrate past its depth of equal density and so entrain denser waters from below and distribute them throughout the mixed layer. This problem of the proportion of kinetic energy that may be utilized to produce penetrative convection has remained unresolved in this context, but has been estimated at about (3.6 ± 3.1)% by Farmer (1975) in his studies of downward thermal convection induced by radiative heating of waters beneath the ice cover on a lake.

The upper convectively mixed layer is separated from lower waters by a sharp pycnocline and into this system comes energy associated with tidal fluctuations and/or atmospheric pressure differences in the outside seas. The response is the subject of this paper.

2. Cambridge Bay

Cambridge Bay (Fig. 1) has been the subject of a number of papers, the most recent of which is due to Gade *et al.* (1974, hereafter referred to as G74). The Bay, of maximum depth 83 m, is connected to the open sea by a shallow channel of length about 8 km between the sills AA and BB shown on the figure. Freeze-up is usually complete by mid-October and the ice breaks up in June with remnants moving about within the bay until the second half of July. Runoff from the river during the summer causes a distinct fresh water layer to exist on the bay surface which moves according to the wind direction (G74). The volume of runoff is greatly reduced by early September and fall gales cause partial mixing of the upper part of the water column and a consequent rise in surface salinity.

Just prior to freeze-up, in addition to wind mixing, convection caused by the cooling of the water surface causes a very complex vertical temperature structure to exist. At some date in the fall all available sensible heat has been extracted from the surface mixed layer; sea ice begins to form and saline convection commences.

0022-3670/78/0873-0880$05.00

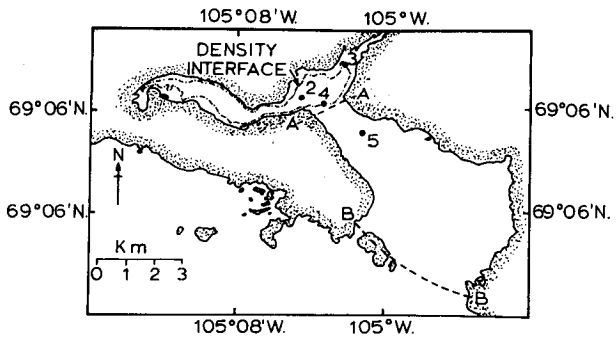

FIG. 1. Cambridge Bay, N.W.T., showing the position of sills AA (depth 17 m) and BB (depth 12 m) at the entrance. The numbers mark the location of experimental sites. The significance of the contour labelled "density interface" is explained in the text.

Seasonal changes in the water structure in Cambridge Bay caused by this mixing are shown in Fig. 2 from G74. The lowering of the prominent temperature "nose" as the season progresses, shows the gradual etching away of heat stored in the water column from the previous summer. The depth of the limit of convective mixing is shown by a sharp salinity change, producing a two-layer system bounded by the ice sheet and the bottom of the bay. As density is dominated by salinity at these temperatures it is seen that there are only minor density variations within the waters of each layer. The December–April increase in upper layer salinity has been shown by G74 to be due to both the salt released by ice growth and that supplied by upward mixing from the lower layer.

Fig. 3 shows temperature and salinity data from the lower layer taken from G74 supplemented with our observation from February 1974. It is noted that although temperature and salinity values are different in the different years, nevertheless, the extensions of all the *T-S* curves intersect the freezing line near a salinity of 29.65‰. G74 interpreted this, and the way in which the *T-S* curve changed during the period of ice growth, as indicating an input of deep convecting water of salinity 29.65‰ at freezing

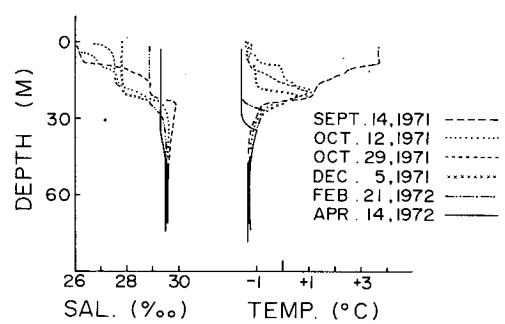

FIG. 2. Seasonal changes in water column temperatures and salinity in Cambridge Bay, N.W.T., winter 1971 (from Gade *et al.*, 1974).

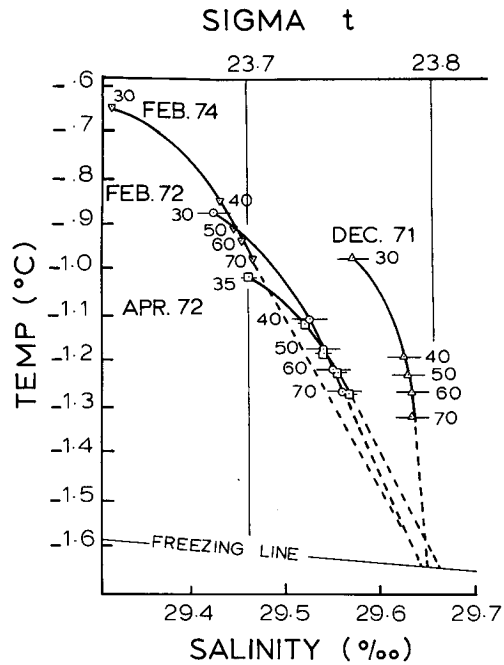

FIG. 3. *T-S* diagram of water in the lower layer of Cambridge Bay for selected months in 1971, 1972 and 1974. Numbers on each curve indicate depth in meters. Note intersection of extensions with freezing point line at about 29.65‰, indicating a "source" water of that salinity.

point. This water is considered to move downward and laterally from the shallows where convection due to salt rejected from the ice sheet cannot penetrate vertically to the full depth of the upper mixed layer. Depending on topography and local currents the resulting salt excess in the shallows can give rise to a density current. On passing through the upper mixed layer which is also at freezing point it could then acquire, on average, the salinity value characterizing the deep convecting water before entering the lower layer. Such a density current would penetrate, mixing as it went, to the depth at which its density matched that of its surroundings before slowly spreading horizontally. The depth contour of the interface between the two layers is shown in Fig. 1. This divides the shallows of the bay, which are a source of this water, from the basin which receives it.

3. Instrumentation

Results to be described are derived from measurements made with a model 8101A Guildline CTD, an Aanderaa current meter equipped with a temperature sensor, and an ultrasonic current meter developed by T. Gytre at the Christian Michelson Institute in Bergen, Norway. The oceanographic sledge used for instrument deployment from sea ice has been described by Lewis (1971). The details of calibration and use of thermistors and checkout pro-

cedures for the CTD are the subject of Lewis and Sudar (1972). In the present instance, where small differences in salinity are of considerable importance, the bench salinometer used to provide standardization for the CTD was, in addition to the usual calibration at 35‰, calibrated using samples having values around 29‰ produced by dilution by weight of Copenhagen water. This salinity is a typical value found in the upper layer of Cambridge Bay. A series of experiments were conducted at various CTD lowering rates and the optimum speed was found so as to match the sensor time constants with sensor position on the instrument frame and scanning sequence of the recorder. The CTD unit was fitted with a tripod so it could be allowed to hit the bottom at the selected speed of 0.8 m s^{-1} without sustaining damage to the sensors. This allowed profiles to be taken down to 0.40 m from the bottom. All eight CTD calibrations done during the two-week experimental period are consistent within ±0.002°C and ±0.008‰ salinity.

As the earth's horizontal magnetic field is insufficient to give a directional reference, the Aanderaa current meter was used without its vane assembly. It was fitted with a tripod so that the rotor and temperature sensor were 0.5 m above the seabed. The latter had a time constant of about 2 min and a resolution of ±0.02°C, a limitation imposed by the 10 binary bit recording system.

The ultrasonic current meter has been described by Audunson *et al.* (1974). It operates on a travel time difference principle between opposed acoustic sources and gives both x and y components of velocity. Currents were obtained either by suspending this meter at various depths from a double armored cable or by resting it on the bottom in its fitted tripod mount with the probes 0.33 m from the bottom. Current profiles were obtained by lowering at dead slow speed (~0.05 m s^{-1}). This mode of operation was made possible by the stable platform provided by the sea ice and the weak currents encountered in these studies. The maximum depth of such a profile was 45 m. While the current meter hung at a fixed depth the orientation of the x and y pairs of transducers, although unknown, did not alter as was demonstrated by rotating the cable 180° to produce an exact reversal and recovering the original reading when the cable was released; the double armor had sufficient torsional rigidity to prevent significant angular oscillations. This same technique was also used to check the zero of the current meter which could vary over periods of several hours. Due to the shielding effect on currents of the four transducers there is a correction to be applied for the non-cosine response of the instrument which will be minimal at the low current speeds encountered in Cambridge Bay and, in any case, would not exceed 10%. No such correction has been made for the present data as our water tunnel tests were made at considerably higher speeds.

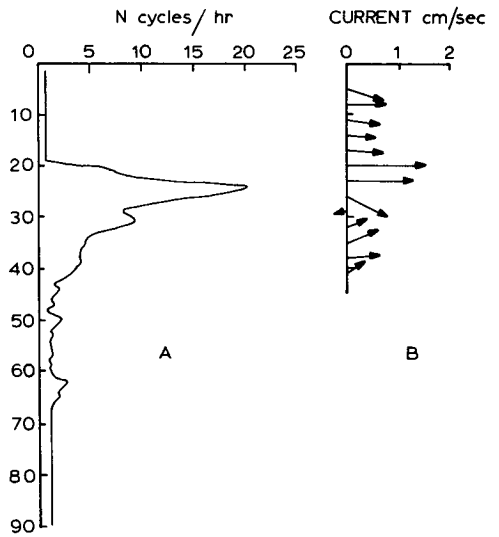

FIG. 4a. Brunt-Väisälä frequency as a function of depth. Values below 1 cycle h^{-1} have been neglected as within the instrumental "noise". 4b. Stick diagram of currents at site 3 (see Fig. 1) as a function of depth. The reversal noted at about 30 m on the interface between the upper and lower layers implies the existence of an internal wave. The total currents are thus a combination of barotropic and baroclinic components. The entire profile was taken within 15 min.

4. Results and discussion

The observational program was designed to look for boundary currents and was not optimal in terms of the physical processes that were actually observed. Fortunately, the sensitivity of the instruments allowed interpretation of data though they were not placed in the best positions. Fig. 4a shows the Brunt-Väisälä frequency profile from CTD readings taken at site 2 (Fig. 1). Apart from nonsystematic variations in the depth of the density step this profile was generally the same for all sites in the bay. Fig. 4b shows a current profile taken at site 3 by the ultrasonic current meter. Superimposed on a barotropic flow is a baroclinic component sufficiently strong to produce a current reversal below the thermocline. Insufficient data were taken to resolve the modal structure of this current but a 15 h time series taken subsequently at the depth of the current maximum showed a strong tidal variation combined with considerable energy at periods of the order of 1 h. During this 15 h period, the current direction stayed in the same quadrant suggesting a net circulation in the bay driven by the tidal current. Such a net circulation could be caused by the deflection of an incoming tidal current by a combination of geostrophic and topographical effects coupled with currents associated with the internal

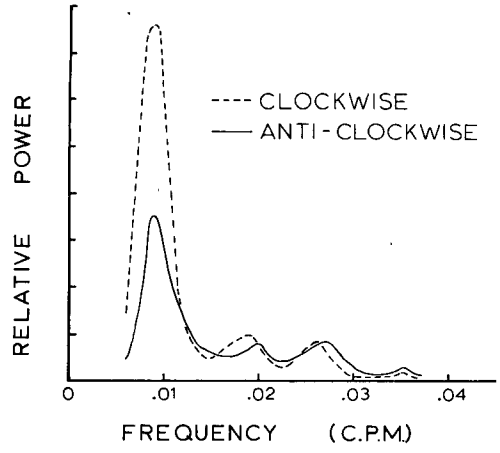

FIG. 5. Rotary power spectrum of water movement near the sea bed at site 3 (see Fig. 1) with the dominant semidiurnal tide component removed. The clockwise peak at ~0.01 cpm corresponds to an energy of 1.4×10^{-7} (m s^{-1})^2 cpm^{-1}.

modes of oscillation. A numerical model based on observations far more extensive than those reported here would be necessary to fully describe such a system, but the net circulation observed should greatly aid horizontal mixing.

A 3½-day ultrasonic current meter record was made with the instrument standing on its tripod on the seabed at site 3. This, in practice, also provided our best record of the internal wave system. The spectrum of this record is shown in Fig. 5. The tidal component was removed in order to show the contribution from the higher frequency internal modes where significant energy is shown close to 0.01 cycle per minute (cpm) (period 1.8 h). The relative amplitude of the harmonic components at about 0.02 cpm and about 0.03 cpm is probably contaminated by the procedure used to remove the power at tidal frequency, and in addition the shape of the current waveform near the seabed may well not be sinusoidal (Cairns, 1967) so that interpretations of the harmonics is not attempted. The rotation

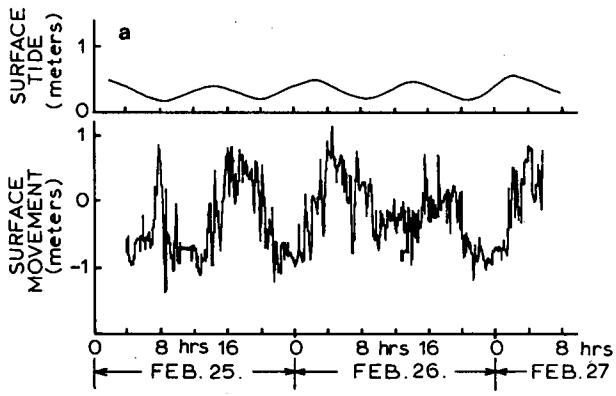

FIG. 6a. Inferred vertical movement of the interface from thermistor chain record at site 3 compared to the tidal cycle.

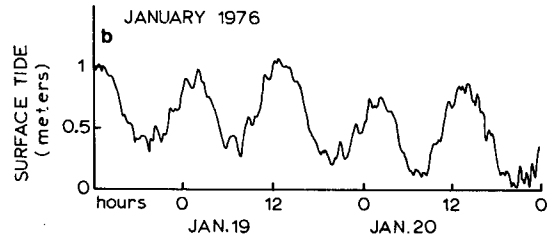

FIG. 6b. Tides in Cambridge Bay showing energy with period about 1.6 h.

of the current vector was predominantly clockwise. Such current ellipses can be related to many causes but for readings taken so close to the bottom and in the presence of a considerable bottom slope, topographic effects probably dominate.

While this record was being taken, temperatures in the vicinity of the interface between the layers were being recorded by a thermistor chain. From these measurements the vertical movement of the interface may be inferred from knowledge of the temperature gradient. This is shown in Fig. 6a together with the tidal record from the float gage maintained at the Cambridge Bay pier. It is seen that superimposed on the displacement of the interface associated with the tidal period are oscillations of a few hours period corresponding to the spectral peaks of Fig. 5. The tidal record of Fig. 6a is shown for comparison of phase only, as it is almost certain that this gage was "sticking" at times so that on occasion it produced an apparently smoothed trace with instantaneous jumps in water height. However, when operating freely, it showed evidence of higher frequency oscillations. The float gage was replaced by a superior instrument in 1975 and 1976 and records throughout these two years show a large component of energy of period about 1.6 h. A section of the January 1976 tidal record is shown in Fig. 6b. This segment has been selected to show a large amplitude 1.6 h period wave; an average amplitude of about half that shown persists throughout the entire year and so we assume that similar fluctuations existed in February 1974, the time of our experiment. During the summer of 1977 records of tides in Cambridge bay showed the usual 1.6 h fluctuation but these were not seen by a gage installed outside the bay about 350 km west in Coronation Gulf; neither were they seen at Coppermine 450 km west of Cambridge Bay. The gage at Spence Bay about 460 km to the east did show high-frequency fluctuations in water height of period about 1 h. We therefore assume that the source of these oscillations lies in the system of channels to the east of Cambridge Bay. It is considered that these fluctuations, an energy source for the internal waves in the Bay, are the result of surface seiches in the channels of the Arctic archipelago.

Simultaneous records of currents and temperature near the interface were examined. Maximum currents of tidal frequency were associated with a maximum thickness of the upper layer. This phase relationship corresponds to that expected for a progressive internal wave which suggests that very little of the internal tide is reflected, a finding in accord with the observations of Gade (1970) working in Oslo fjord. According to LeBlond (1966) the 1.8 h period oscillations can be expected to propagate for about five times as many cycles at the tidal period wave for small values of eddy viscosity. Therefore, in a bay with dimensions suitable for a standing wave of both frequencies, the 1.8 h period wave could give rise to a seiche, while the tidal period wave dissipates. The velocity v of the lowest mode of wave propagating in a two layer system is given by

$$v = [g\Delta\rho H_0 h_0/\rho(H_0 + h_0)]^{1/2}, \quad (1)$$

where ρ is density (1020 kg m^{-3}), $\Delta\rho$ the density difference between layers (0.7 kg m^{-3}), g the gravitational acceleration (9.8 m s^{-2}) and H_0 and h_0 are the upper and lower layer thicknesses (22 and 24 m). The values in parentheses are those suitable for Cambridge Bay, where 24 m has been taken as the average lower layer thickness of the basin immediately opposite the sill AA. The Rossby radius ($R_0 = v/f$, where f is the Coriolis parameter) for the internal modes of oscillation is of the order of 2 km so the basin of Cambridge Bay can be treated as a narrow channel without rotation for these calculations. For a period of 1.8 h this formula gives 900 m for a half-wavelength which is in good agreement with the measured width of the basin behind sill AA at the depth of the interface. This mode of oscillation is near resonance with the surface fluctuations of 1.6 h period noted on the tidal record and so may be able to extract energy from this source to support a seiche. Fig. 7 shows a portion of the record from the Aanderaa current meter at site 4, just inside sill AA. It was positioned on the bottom at a depth of 34.5 m, well below the interface. Although the temperature record showed the continual presence of the 1.8 h period fluctuations, the current meter threshold was exceeded only for two intervals, each of about 12 h. Fig. 7 is the record for one of these intervals showing a strong signature of 1.8 h period. At the 34.5 m level temperature decreases with depth so Fig. 7 shows that the current pulses are associated with a downward movement of water. Any upward water movement is still below threshold values.

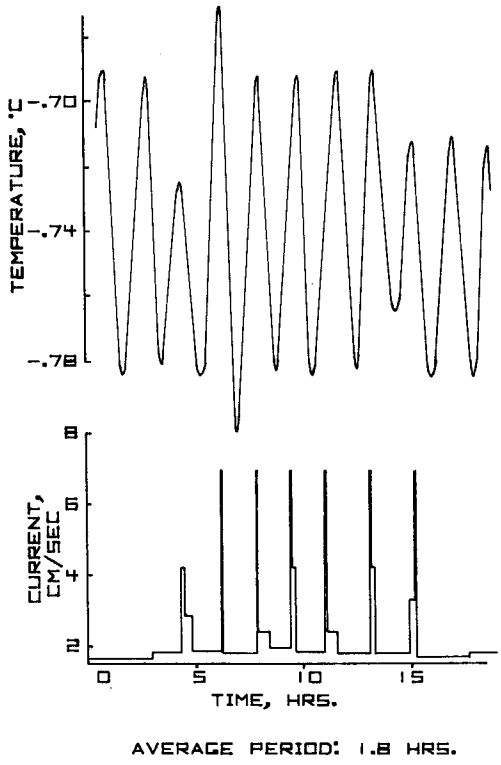

FIG. 7. Current and temperature records just below the layer interface within the bay near sill AA (site 4, Fig. 1). The current is below threshold value for most of the time. Temperatures have been smoothed from 0.02°C steps dictated by the 10-bit binary recording system.

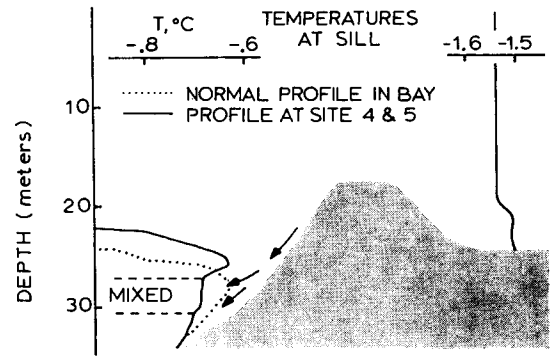

FIG. 8. Temperature profiles just within and without the sill AA (site 4, Fig. 1) compared to the "normal" profile typical of the interior of the bay. The thermocline height varies according to the phase of the internal wave so that the about 2 m difference in depth at the temperature "nose" has no significance.

Fig. 7 is best interpreted in conjunction with Fig. 8 which shows temperature profile from CTD observations at ¼ m depth intervals from just within and without the sill and also the "normal" temperature profiles taken from a record in the center of the bay. It is noted that just under the temperature maximum a new mixed layer has been formed which is attributed to surges of current moving up and down the slope; the internal seiche is breaking and the downward surges are much stronger than the upward ones. The site 5 profile shows a small degree of warming near the bottom, possibly due to exchange over the sill as a result of runup. Fig. 9 shows the record from an ultrasonic current meter

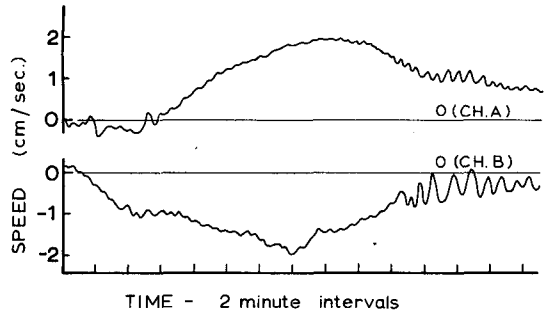

FIG. 9. Ultrasonic current meter record at site 4 (Fig. 1). Channels A and B are the outputs giving orthogonal velocity components in a plane parallel to the sea bed. A typical event from a 17 h continuous record is shown. Similar events occurred every 1.8 h though with varying amplitude.

placed at site 4 at a later time. The downward movement of water recorded in Fig. 7 can be seen in much greater detail. "Blobs" of water are moving down the slope with increasing turbulence apparent in their wakes. Although it can have many causes this turbulence is a necessary feature of gravity flows as was shown by Benjamin (1968). Such surges in shallow waters have been reported by Winant (1974) and breaking processes have been studied by Cacchione and Wunsch (1974). However, the latter authors considered a continuously stratified medium which makes their results inapplicable to the present case. Stigebrandt (1976) conducted some laboratory experiments showing complete degeneration into turbulence of internal waves impinging on a sloping bottom at an interface between fresh and salt water but, as he has pointed out, these results cannot be scaled up to apply to nature as the process is nonlinear. Temperature readings were taken by the Aanderaa instrument every 5 min for 11½ days and from this complete temperature record, a portion of which has been shown in Fig. 7, the spectrum of Fig. 10 is obtained. Prominent are peaks at tidal and at 1.8 h periods, with the energy being dissipated at the higher frequencies according to a power spectrum law with a logarithmic slope close to $-5/3$.

Stigebrandt (1976) also published an analysis of internal waves of tidal frequency excited in a fjord by tidal movement over the interface between an upper brackish layer and the basin water at the depth of the sill. By matching the barotropic mode with the internal tide propagating away from the sill on the interface between layers he derived equations for the amplitude η and energy flux ϵ of the internal tide at the sill, i.e.,

$$\eta = \alpha h_0 / v, \tag{2}$$

$$\epsilon = \tfrac{1}{2}\rho\alpha^2(h_0^2/H_0 + h_0)vB, \tag{3}$$

where

$$\alpha = \frac{2\pi AY}{TB(H_0 + h_0)}, \tag{4}$$

Y is the surface area of the fjord inside the sill, A the amplitude of the surface tide of period T, and B the width of the channel. The use of suitable values for Cambridge Bay allows prediction of an amplitude of 0.82 m for the internal tide and an energy flow of 6.8×10^2 W into the Bay past sill AA. The amplitude agrees very well with that measured at site 3 and shown in Fig. 6a, which is to be expected as the time taken for the internal tide to propagate from the sill to site 3 is very short compared to the period.

Taking an amplitude for the 1.6 h surface oscillation from the tidal records would enable a similar calculation to be made for the energy input at this period provided an assumption is made regarding the proportions of standing and traveling waves in the 1.8 h internal seiche and the "bandwidth" of the Bay's response. LeBlond (1966) estimates that waves of this period dissipate within a few cycles in shallow water. Taking an amplitude of 0.0725 m at 1.6 h from the tidal record and assuming, for argument, that half the energy generated at the sill is dissipated in each cycle the estimated energy input to the internal seiche is 10^3 W, more than that contributed by the internal tide. The computed amplitude at 1.6 h period at the sill is 1.40 m. Taking the temperature gradient just above the bottom at site 4 as -0.018°C m^{-1} allows the temperature oscillations of Fig. 7 to be interpreted as an excursion of ± 2.20 m at 1.8 h period. Away from the sill, where the wave is not breaking, the amplitude is much smaller as can be seen from the plot of the interface displacement at site 3 (Fig. 6). For comparison the potential energy of the salt rejected by ice growth at a rate of 1 cm day^{-1} is 3.2×10^3 W which is mainly dissipated as turbulence in the upper layer.

It is possible to consider the density profile of the Bay as a combination of constant (upper layer) and exponential (lower layer) variations with depth

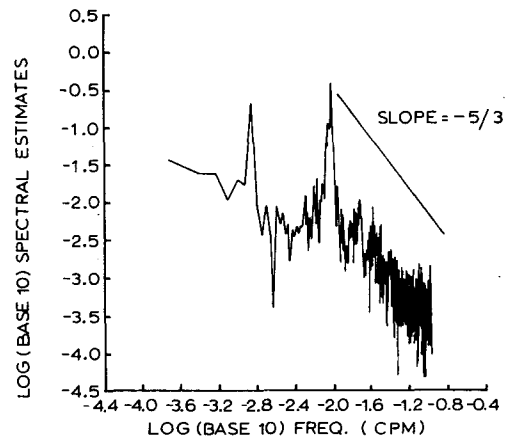

FIG. 10. Spectrum of temperature fluctuations recorded at site 4 (Fig. 1).

and make a fit allowing determination of the constants α, β and γ in the expression $\rho = \alpha[1 + \beta \exp(-\gamma z)]$. This was done and the dispersion relation for internal waves in a bay of appropriate constant depth was determined following Garrett and Munk (1972). Solutions for the vertical and horizontal velocities associated with a given amplitude and period of oscillation follow so that the profile of the Richardson number

$$\mathrm{Ri} = -g \frac{\partial \rho}{\partial z} \Big/ \rho \left(\frac{\partial u}{\partial z}\right)^2 \qquad (5)$$

may be calculated for the lower layer, where u is the horizontal velocity associated with the internal wave. For Ri < ¼ mixing will occur taking energy from the wave. In the upper layer, where $\partial\rho/\partial z = 0$, energy loss from shear instability mixing will be limited to viscous dissipation and should be much less than that associated with mixing of the density gradient in the lower layer.

On the basis of the above analysis it was found that mixing would be most likely in a thin layer immediately below the interface of thickness 1.5 m where all internal modes at tidal and 1.8 h period are relatively unstable. Instability of this kind depends on the amplitude and mode of the internal wave. For our measured values of interface displacement the first mode would be stable and we consider that by far the greater portion of the energy available from the internal waves is dissipated during breaking along the "density interface" contour of Fig. 1. In the absence of convecting saline waters from the shallows, the mixing caused by breaking internal waves would form a water of intermediate density which would move outward from the density interface contour toward the center of the bay. In the presence of the convecting 29.65‰ water at freezing point, breaking internal waves would modify the existing density current as it penetrates to the bottom of the bay. Most of the internal wave energy would be dissipated in the lower layer.

The straight line T-S relationships of Fig. 3 indicate that the lower waters of the bay are being mixed at all times. The potential energy difference between the observed density profile and a completely mixed lower layer was calculated to be 25 $\times 10^8$ J. From the above calculations this amount of energy would be generated about every 17 days by the baroclinic modes at the sill; maybe 5% of this energy would be available to do work mixing against gravity.

Fig. 11 shows the rate of change of salinity in the upper mixed layer of Cambridge Bay and in the channel between sills AA and BB. It is noticed that the rate of change of 0.01‰ day^{-1} is associated with a salinity difference of 0.04‰, the bay having the higher value. Since the mixed layer inside sill AA is

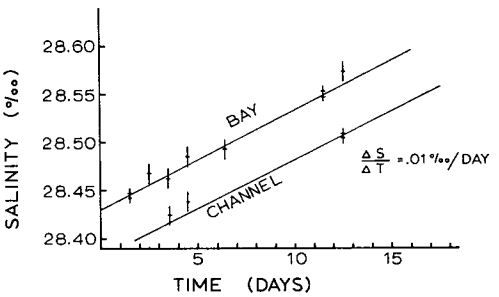

FIG. 11. Rate of change of salinity of the upper layer within the bay and between sills AA and BB (Fig. 1). Bars indicate limits of accuracy of the measurement.

deeper than the shallows, uniform salt rejection would be expected to produce a salinity excess in shallows far enough from the bay to not participate in deep water convection. The fact that the salinity excess occurs inside the bay is evidence of dominant effects of upward entrainment of salt from the lower layer and is in accord with the observed seasonal overall reduction in salt content of the lower layer in spite of the input of deep convecting water. Turbulence in the upper layer due to salt rejection by ice growth is greatly in excess of that in the lower layer caused by shear-induced mixing so that except at the boundaries entrainment will be the dominant mechanism for upward salt flux.

6. Conclusions

An ice-covered Arctic bay is a two-layered system with energy inputs from water level changes and salt-driven convective processes. In the upper layer convective processes will produce an accumulation of salt in the shallows causing a density current to run down slopes and impinge on the density interface at the convective limit. Internal waves at frequencies associated with the external forcing function at the fjord sill exist on the interface at this convective limit and the breaking of these waves on the shores of the bay modify the density currents as they move downwards into the lower layer. Mixing occurs down the slopes of the bay to the bottom and produces small horizontal density gradients within the lower layer that themselves contribute to the mixing process. Entrainment upward from the more saline lower layer into the upper layer occurs at the interface giving the latter a salinity within the bay greater than that external to it. What evidence there is indicates that little of the waves are reflected from the shallows and the greater part of their energy is available for mixing. In arctic fjords, where wind mixing is unimportant during the greater part of the year, this mechanism for solute transport between the upper and lower levels of the bay will probably be the most important in determining vertical movement of a pollutant. Spectral analysis of tidal records within and without the

bay, together with some knowledge of the amplitude of internal waves on the interface between the two layers, would normally enable one to make some estimate of the energy available for mixing the lower levels in terms of the density gradient existing therein and the local bathymetry. Upward diffusion of salt from the basin waters is aided by the internal wave field which then, to some extent, must control the frequency with which the basin water is replaced from outside. As short-period oscillations in water height are common in estuarine waters with a complex local topography and as run-off from the land produce a two-layer system similar to that analysed here for Arctic fjords, it is probable that the mechanism of breaking of internal waves coupled to surface waves at tidal and higher frequencies plays a significant role in vertical mixing in fjords at all latitudes.

Acknowledgments. The insight gained during many discussions with Dr. D. M. Farmer of this Institute was most helpful to us. It is a pleasure to thank him for making his knowledge and experience so freely available to us.

REFERENCES

Audunsun, T., T. Gytre and A. Laukholm, 1974: Measuring fluid flow by an acoustic velocity meter. Unpublished report, River and Harbour Laboratory, Trondheim, Norway, 26 pp.

Benjamin, T. B., 1968: Gravity currents and related phenomena. *J. Fluid Mech.*, **31**, 209–248.

Cacchione, D., and C. Wunsch, 1974: Experimental study of internal waves over a slope. *J. Fluid Mech.*, **66**, 223–239.

Cairns, J. L., 1967: Asymmetry of internal tidal waves in shallow coastal waters. *J. Geophys. Res.*, **72**, 3563–3565.

Eide, L. I., and S. Martin, 1975: The formation of brine drainage in young sea ice. *J. Glaciol.* **14**, 137–154.

Farmer, D. M., 1975: Penetrative convection in the absence of a mean shear. *Quart. J. Roy. Meteor. Soc.*, **101**, 869–891.

Gade, H. G., 1970: Hydrographic investigations of Oslo fjord, a study of water circulation and exchange processes. Rep. 24, Geophys. Inst., University of Bergen, 193 pp.

——, R. A. Lake, E. L. Lewis and E. R. Walker, 1974: Oceanography of an Arctic bay. *Deep-Sea Res.*, **21**, 547–571.

Garrett, C., and W. Munk, 1972: Space-time scales of internal waves *Geophys. Fluid Dyn.*, **2**, 225–264.

Kraus, E. B., and J. S. Turner, 1967: A one-dimensional model of the seasonal thermocline. II. The general theory and its consequences. *Tellus*, **19**, pp. 98–106.

Lake, R. A., and E. L. Lewis, 1970: Salt rejection by sea ice during growth. *J. Geophys. Res.*, **75**, 583–597.

LeBlond, P. H., 1966: On the damping of internal gravity waves in a continuously stratified ocean. *J. Fluid Mech.*, **25**, 121–142.

Lewis, E. L., 1971: The collection of oceanographic data from the sea ice surface in winter. *Proc. First Inter. Conf. Port and Ocean Engineering Under Arctic Conditions*, Vol. 2, Technical University of Norway, Trondheim, 1219–1224.

——, and R. B. Sudar, 1972: Measurement of conductivity and temperature in the sea for salinity determination. *J. Geophys. Res.*, **77**, 6611–6617.

Stigebrandt, A., 1976: Vertical diffusion driven by internal waves in a sill fjord. *J. Phys. Oceanogr.*, **6**, 486–495.

Winant, C. D., 1974: Internal surges in coastal waters. *J. Geophys. Res.*, **79**, 4523–4526.

Zubov, N. S., 1943: *Arctic Ice* (English translation). U. S. Navy Electronics Lab, San Diego, 491 pp.